Growth strain assessment at the periphery of small-diameter trees using the two-grooves method: influence of operating parameters estimated by numerical simulations

Delphine Jullien, Joseph Gril

Growth strain assessment at the periphery of small-diameter trees using the two-grooves method: influence of operating parameters estimated by numerical simulations

Delphine Jullien, Joseph Gril

Abstract The two-grooves method used for estimating the surface locked-in strains on standing stems was studied using a finite-element model simulating the gauge measurement resulting from the groove cutting, having in mind the particular of small diameter trees. The assumed growth stress distribution was described by simple polynomial expressions of the relative radius with the possible existence of a tension wood sector characterized by higher residual stresses in the longitudinal direction. The end effect of the crosscutting vanished for a height/diameter ratio higher than 3 and the simulated gauge measurement reasonably approached the local growth strain average. For very small trees with a diameter of about 2 cm, the distance between gauge end and groove should not exceed 3 mm, a value of up to 5 mm is allowed in case of larger stems, 5–20 cm. For any combination of stem diameter, gauge length, groove distance and depth, and assumptions on the internal stress distributions, the underestimation of the surface growth strain by the gauge can be evaluated using the developed numerical tool.

Introduction

Trees control the orientation of their stems, and improve their flexibility by the production of residual stresses in the newly deposited wood layers (Wilson and Archer 1979). The biochemical processes responsible for the generation of these so-called growth stresses during cell-wall maturation are not fully understood. However, their technological consequences can be considerable for the utilization of the wood material. They include log-end splitting after crosscutting, and board distortion or cracking. These phenomena which sometimes result in heavy loss are

D. Jullien (✉) · J. Gril
Laboratoire de Mécanique et Génie Civil, UMR 5508, CNRS-Université Montpellier 2,
Place E. Bataillon, cc 048, 34095 Montpellier CDX 5, France
e-mail: jullien@lmgc.univ-montp2.fr

triggered by heating operations applied during secondary transformation due to the recovery of locked-in growth strains (Kübler 1987). With the considerable development of fast growing tree plantations, a better knowledge of the growth stress distributions in tree stems is essential for ensuring an acceptable quality of wood production in the future.

The assessment of growth stresses usually relies on peripheral measurements performed at different angular positions around the stems (Archer 1986). The relative displacement consecutive to a cutting allows for estimation of the locked-in growth strain, from which the growth stress can be obtained based on the knowledge of the elastic behavior of the material. The few available methods are examined and compared in Fournier et al. (1994) and Yoshida and Okuyama (2002). The single-hole method such as developed by CIRAD, France, allows the quickest evaluation and is thus most appropriate for the rapid assessment of a forest stand. The measured displacement, however, relates to the peripheral longitudinal growth strain through a coefficient depending on the tangential anisotropy and it is influenced by the distribution of material properties and residual stresses in the drilled zone; moreover, it is subject to perturbations resulting from misalignments of the pins (Sassus 1995). In the case of small diameter trees, such a method designed for medium or large diameters can hardly be used, and the two-grooves method seems more appropriate. Although more time-consuming and requiring more expensive equipment, it provides a local strain measurement related in a straightforward way to the locked-in growth strain. However, the practice of the field and the analysis made in Jullien et al. (2006a, b) show that several operating parameters can influence the measured value and need to be properly established to avoid a loss of precision: distance between the two grooves, length of the strain gauge, depth of the grooves… The objective of this paper is to quantify their influence on the measured strain in the case of "small" stem diameters ranging from 20 to 200 mm, and to make recommendations for the field practice. As the inner growth stress distribution should obviously have some influence, they will be also considered by various assumptions on the radial profiles and tension wood occurrence.

Numerical model

The two-grooves method, used to evaluate maturation strain at the periphery of a stem, is commonly performed on a standing tree (Yoshida and Okuyama 2002). The bark is removed around a portion of the stem at breast height. In the basic "strain gauge method" several strain gauges (typically 2, 4 or 8, depending on the stem diameter) are glued at a given height, all around the stem, aligned with the stem axis. Two grooves are made horizontally up and down each gauge until the signal of the gauge is stabilized. The longitudinal strain released by cutting is recorded for each gauge. Figure 1 shows the principle of the method and indicates the geometrical parameters. In this work, a finite element model was developed to simulate the two-grooves method applied at one position of the stem. Calculations were conducted using the finite element code CASTEM. The trunk was modeled as

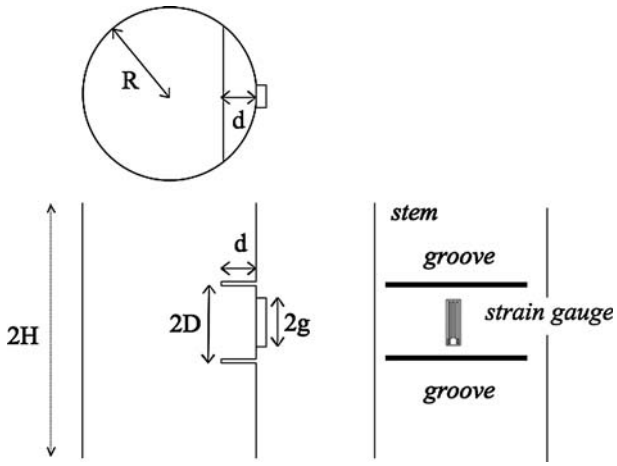

Fig. 1 Geometrical parameters of the two-grooves method. *d* groove depth; *D* half distance between the two grooves; *g* half length of the gauge; *R* stem radius; *H* half log height

a cylinder; the horizontal symmetry plane allows for meshing only the half-length of the log, and only one groove. The upper part of the cylinder, above the groove, is necessary to avoid edge effects: its minimal length *H* will be discussed in the results. The thickness of the groove, described by a portion of a horizontal section at distance *D* from the mid-plane and with a varying depth *d*, was neglected. Each node of that cross-section was doubled and the sawing of the groove was simply simulated by allowing the relative movement of corresponding nodes.

The wood in the stem was considered as cylindrically orthotropic: the radial (R), tangential (T) and longitudinal (L) directions follow the cylindrical coordinates (r, θ, z), and the transverse (RT) and radial (RL) planes constitute two orthogonal planes of material symmetry. The values of elastic constants used for the simulations were obtained using empirical equations established by Guitard (1987) for a typical hardwood with a density of 0.65 g/cm^3 and a moisture content of 30%, see Table 1. The principle of the calculation is that an initial residual stress field σ^i is assumed to exist in the standing tree; when the free surface (the groove) is created, a displacement field results, and one obtains the predicted gauge measurement as the relative displacement of the node corresponding to the upper end of the gauge. In the case of unbalanced stress field σ^i over the cross-section, its application induces an initial bending of the stem; the resulting displacement field (calculated for a groove depth $d = 0$) must be subtracted to correctly simulate the measurement.

Table 1 Constants used for the simulation

Moduli (MPa)						Poisson's ratio			Stress field (MPa)			
E_R	E_T	E_L	G_{LR}	G_{RT}	G_{LT}	ν_{LR}	ν_{RT}	ν_{LT}	q	p_1	p_2	k
833	474	10,512	580	168	447	0.61	0.67	0.73	−0.61	10.06	0 or 2.p_1	1

At the stem periphery a state of plane stress is assumed, so that the T and L components of the residual growth stress σ^{i} are related to those of the locked-in strain α by:

$$\sigma^{i}_{L} = -E_{L}[\alpha_{L} + \nu_{TL}\alpha_{T}]/(1 - \nu_{LT}\nu_{TL}); \quad \sigma^{i}_{T} = -E_{T}[\alpha_{T} + \nu_{TL}\alpha_{T}]/(1 - \nu_{LT}\nu_{TL}). \tag{1}$$

The initial growth stress in the standing tree is supposed to be independent of the axial coordinate z. The transverse components are "axisymmetric", which means that they are independent of the angular position, and given as a function of the relative distance to pith r/R by:

$$\sigma^{i}_{R}(r) = q\left[(r/R)^{k} - 1\right]/k; \quad \sigma^{i}_{T}(r) = q\left[(1+k)(r/R)^{k} - 1\right]/k \tag{2}$$

where q is the surface strain in T direction, and k a constant. This formulation is a generalization of the model of Kübler (1959a, b), which is obtained when k tends towards 0. When $k = 1$, the stress field is linear with r/R. When $k > 1$, the stress field is more flat in the core of the stem and, by compensation, more rapidly changing close to the cambium. In the L direction, the possible presence of reaction wood is taken into account by adding an asymmetric term so as to fit with peripheral values of residual stresses typically measured on standing trees:

$$\sigma^{i}_{L}(r,\theta) = [p_{1} + p_{2}(\theta)]\frac{(2+k)(r/R)^{k} - 2}{k} \tag{3}$$

where the constant p_1 is the level of axisymmetric part (independent of the angular position) and p_2, that of the additional asymmetric part (a function of the angular position). As a remark, the constant k is directly related to the relative gradient of the stress distribution near the periphery, with the radius r normalized by the stem radius R and the stress σ^{i}_{L} normalized by the surface stress $p_1 + p_2$:

$$\left\{\frac{d}{d(r/R)}\left[\frac{\sigma^{i}_{L}}{\sigma^{i}_{L}(R)}\right]\right\}_{r=R} = 2 + k. \tag{4}$$

The stress distributions considered here represent situations where the direction of up righting movement of the stem has been the same from the beginning, and the growth rate has been regular. To model the case of changing angular positions of the reaction wood zone and/or sudden changes of growth conditions, a ring-by-ring description would be required. A maturation strain of $\alpha_T = 0.2\%$, and $\alpha_L = -0.1\%$ in normal wood, $\alpha_L = -0.3\%$ in tension wood was assumed. Hence q, p_1 and p_2 are calculated from equations (1), (2) and (3), and included in Table 1. p_2 was taken as 0 to simulate the axisymmetric case of no reaction wood. To simulate asymmetric cases, p_2 will be taken as 2. p_1 in an angular sector of 90° corresponds to the tension wood zone and 0 in the rest of the log, corresponds to normal wood. The different stress profiles are illustrated in Fig. 2.

Five positions of tension wood were simulated (Fig. 3).

To better understand the influence of the various parameters on the simulated measurement, many sets of simulations have been conducted. The results are discussed in the next part. Table 2 shows the values given to each parameter for

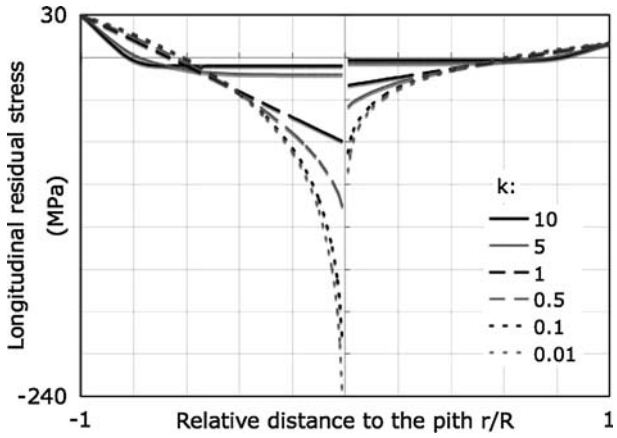

Fig. 2 Longitudinal initial stress profiles, for different values of coefficient *k*

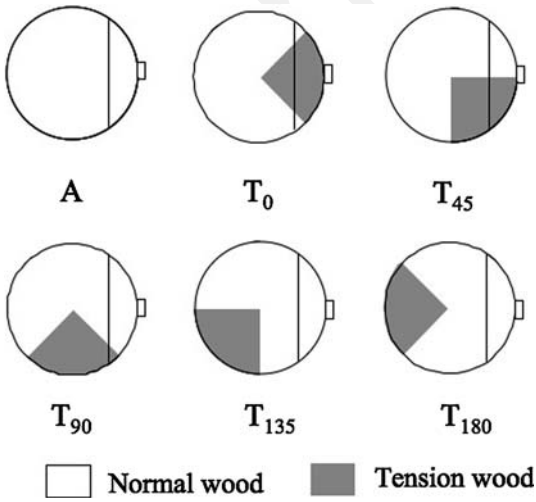

Fig. 3 Distribution of tension wood: *A* axisymmetric case, T_n asymmetric cases with *n* the angle between the groove and the tension wood zone. The *vertical line* indicates the depth of the grooves

each set of simulations. The values in bold character correspond to the varying parameter along the *x* axis, and the ones in italics to the parameters corresponding to each curve.

Results and analysis

Effect of the log height

Although the two-grooves method is usually performed on a standing tree, the finite element model simulates the behavior of a log. This log must be long enough to properly calculate, in its central part, what really happens in a standing tree. The

Table 2 Sets of simulations

R (mm)	*H/R*	*g* (mm)	*D* − *g* (mm)	*D* (mm)	*d* (mm)	*k*	TW occurrence	Figures
10, 25, 50, 100	**0.25–6**	1				1	A	4
25	4	1	5		10	1	**A, T_0– T_{180}**	9
10, 25, 50, 100	4	1	5		10	**0.01–10**	A	10
10, 25, 50, 100	4	*1, 4*	**0.5–50**		10	1	A	11
10	4	**1–5**	*3*		10	1	A	12
25, 50, 100			*5*					
25	4	**1–5**		6	*0.5 ~ 10*	1	A	13
10	4	3	*3*		**0.2 ~ 50**	1	A	14
25, 50, 100			*5*					

R, H, g, D, d: see Fig.1; k: see Eqs. 2, 3; *TW* (tension wood) occurrence: see Fig. 3. Bold characters: varying value; italics: curve parameters

initial stress field σ^i assumed to be locked in the standing tree induces strains in the log. The longitudinal strain is evaluated at the periphery of the stem, assuming that a gauge of length 2 mm is centered at the middle-length of the log, for different lengths of log. These calculations are repeated for different radii of the log. This initial strain becomes constant and reaches 99% of the final value when the upper part is 30, 75, 150 and 300 mm long for stem radii of 10, 25, 50 and 100 mm, respectively (Fig. 4a). These distances correspond to three times the radius of the stem (Fig. 4b). In further calculations, edge effects are avoided by taking an upper part four times as long as the stem radius.

Effect of boundary conditions

Figure 5 shows the deformed shapes due to the initial stress field, and to the relative groove depths of, respectively, 0.04, 0.1, 0.2, 0.4 and 1 in case T_0, for which the two-grooves method was performed on the side of the tension wood zone, on a tree

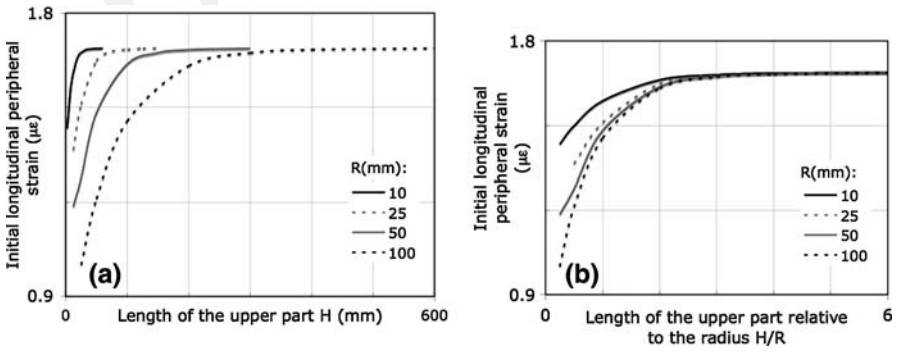

Fig. 4 Initial longitudinal strain function of the length of the upper part (**a**) or the length of the upper part relative to the radius (**b**) for four stem radii with the half-length of the gauge g = 1 mm

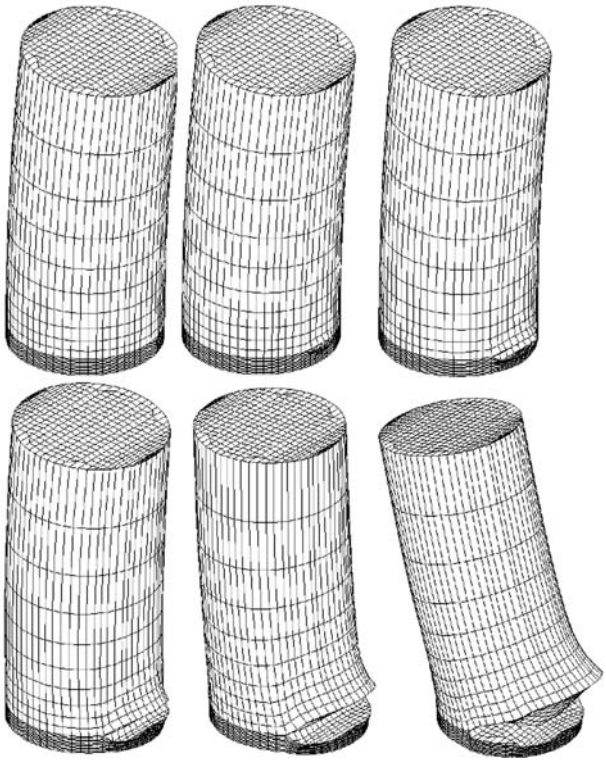

Fig. 5 Deformed mesh for initial stress field, and relative groove depths of 0.04, 0.1, 0.2, 0.4 and 1, respectively, in case of T_0. (the displacement of each node was amplified by 100)

of radius 25 mm. The slight curvature observed on the first mesh results from the initial stress field imposing a bending moment toward the tension wood zone. When the grooving starts, some of the peripheral tensile stress is released, inducing a counter curvature in the central zone of the stem.

Figure 6 shows the corresponding evolution of the longitudinal stress along a central diameter joining the tension wood and the opposite wood sides. Compared to the initial stress profile, linear with respect to the radius ($k = 1$), the cutting caused a rapid fall of the stress in the region comprised between the two grooves, and, by compensation, an increase of the tensile stress in the wood located deeper toward the pith. On the opposite side, it caused a slight stress increase at the start; however, when half of the stem has been cut ($d = 25$ mm) the stress is almost completely released at the periphery.

Figure 7a shows a very similar evolution of stress profiles in the axisymmetric case (A). In all cases, a rotation around the y axis of the upper cross-section on the deformed shape was noticed. Figure 8a shows this movement with a diagram. In Fig. 7b, a different boundary condition has been imposed: the rotation around the y axis of the upper cross-section has been prevented, without, however, preventing its axial movement (Fig. 8b). This would correspond to the situation where the upper

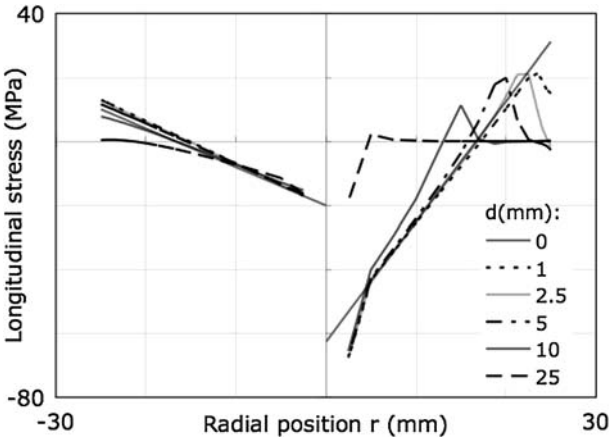

Fig. 6 Longitudinal stress profiles along a central diameter joining the tension wood and the opposite wood sides, in case of T_0, for different groove depths d

part of the stem is maintained during the growth strain measurement, to prevent the perturbation by wind—that condition being naturally imposed, in the bottom part, by the root anchorage. At the start of the grooving, the difference between both stress profiles is small. For the high groove depth values (d), it becomes very obvious, especially on the opposite side where almost no stress decrease is observed when the stem is maintained upright.

In the following simulations, the free boundary conditions, such as shown in Fig. 5, 6 or 7a, were assumed considering that in most cases where the groove depth is only a small portion of the radius, the effect is imperceptible.

The effect of the crown weight has been neglected in this analysis. It is likely to be negligible in the case of larger stem diameter where the relative groove depth is small. In the case of a small diameter tree, it is common practice to cut the crown at a sufficient distance from the measurement zone, thus avoiding the bending perturbations. An alternative could be the clamping of the upper part. In both cases, the present analysis would correctly predict what is measured at the gauge level.

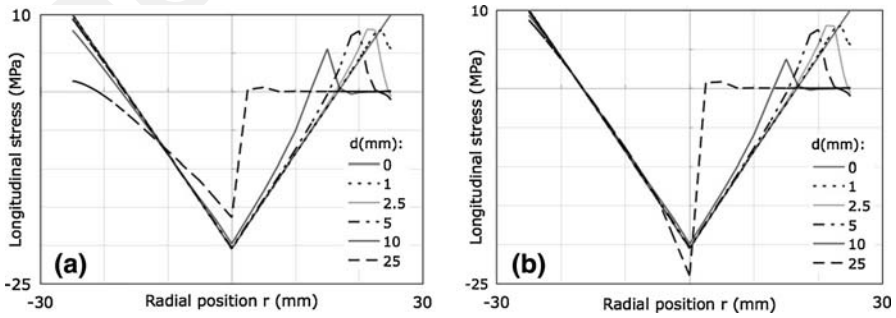

Fig. 7 Longitudinal stress profiles along a central diameter, in axisymmetric case A, for different groove depths d, with free (**a**) or prevented (**b**) rotation of the upper cross-section

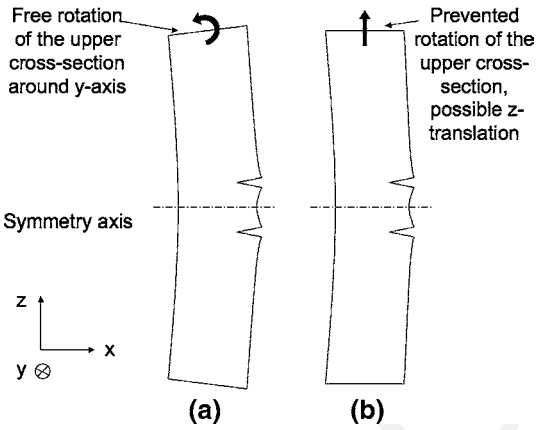

Fig. 8 Boundary conditions: free (**a**) or prevented (**b**) rotation of the upper cross-section

Effect of tension wood

The evolution of the stress profiles in Figs. 6 and 7a shows that, at least at the beginning of the grooving, the opposite part is little affected by the operation. This suggests that, in return, the measurement is not much affected by the mechanical situation in the opposite zone. Now, the effect of the tension wood position on the measurement is studied more generally. As was described above, the tension wood zone is here a 90° sector in which the maturation strain is three times higher than in normal wood. The five cases considered are presented in Fig. 3.

When the grooves are made on the tension wood side (case T_0), the released strain is -0.25% which represents only 85% of the local maturation strain $\alpha_L = -0.3\%$ (Fig. 9). In the case of T_{45}, the released strain, about -0.17%, represents 85% of the mean local maturation strain, which is about -0.2%. In the case of T_{90}, the tension wood zone has no influence on the released strain, its value is very similar to the one obtained in the case of no tension wood. In the cases of T_{135} and T_{180}, the opposite tension wood zone tends to slightly increase the released strain; it represents 115 and 124% of the local maturation strain. Thus, an asymmetric distribution of the maturation strain may influence, to a different degree, the strain measurement all around the tree.

Effect of the internal stress distribution

In all preceding simulations the parameter k describing the internal stress profiles was set to 1. When this parameter was varied for given operating conditions, Fig. 10 shows that the longitudinal released strain is not very sensible to the k coefficient, at least for stem radii R significantly higher than the groove depth d. In the case of relatively small diameters, such as here R = 10 mm for d = 10 mm, the influence was naturally more obvious. In the case of high k values, the influence was also stronger: the peripheral stress was more affected by high k values than by low k values. Low k values led to a released strain close to the maturation strain. This is understandable, considering the fact, shown by Eq. 4, that the stress gradient at the

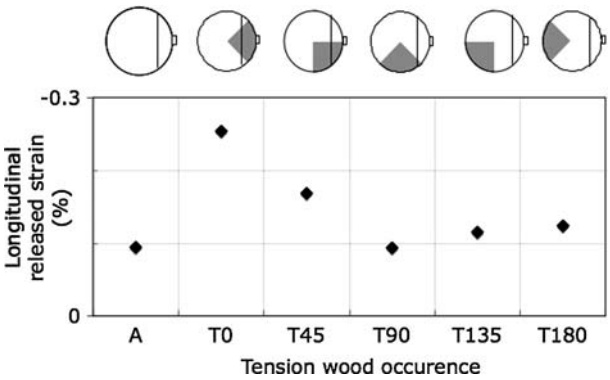

Fig. 9 Longitudinal released strain for different tension wood positions. R = 25 mm, d = 10 mm, $D - g$ = 5 mm, g = 1 mm

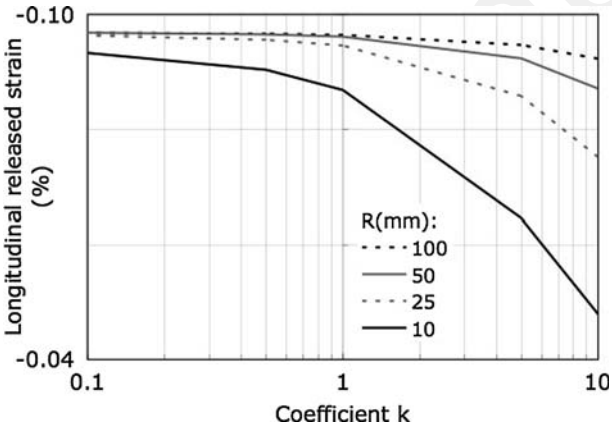

Fig. 10 Effect of the internal stress distribution (parameter k, see Fig. 2) on the longitudinal released strain for different stem radii (R). d = 10 mm, $D - g$ = 5 mm, g = 1 mm

periphery is proportional to $2 + k$: the lower the k, the more homogeneous the stress in the measuring zone. In the case of a high k value, the maturation strain would be largely underestimated, especially for very small stems. In all following simulations, the k value will be set again to 1.

Effect of the distance between the groove and the gauge

For the two-grooves method, a strain gauge is glued at the periphery of the stem. Then, the upper and lower grooves are produced to release the stress of the wood located under the gauge. In principle, the grooves should be made as close as possible to the end of the gauges to give an accurate measurement – although not too close, to avoid the very local compression due to wood sawing (Yoshida and Okuyama 2002). However, sometimes it is not possible to cut very close to the end

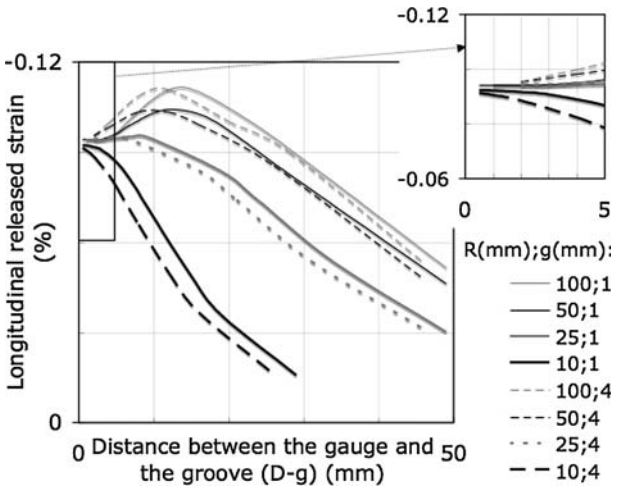

Fig. 11 Effect of the distance between the gauge and the groove ($D - g$) for four stem radii (R). d = 10 mm, g = 1 or 4 mm

of the measuring part of the gauge, because of the attachment of electric wires or other aspects of the gauge design. Now, the effect of the distance between the end of the gauge and the groove on the strain measurement is quantified. In these calculations, the groove depth (d) was 10 mm and the half-length of gauge (g) was either 1 or 4 mm. When g = 1 mm, for the biggest radii, the longitudinal released strain was constant and about 95% of α_L for distances between the end of the gauge and the groove smaller than 5 mm (Fig. 11). For longer distances, the value increased slightly and then decreased with a constant slope relative to the gauge-groove distance. For the 10 mm radius, the released strain started to decrease when the distance $D - g$ was higher than 3 mm. For a longer gauge (g = 4 mm), the released strain for distances $D - g$ smaller than 5 mm was less stable. For longer distances, the value increased and then decreased with a constant slope. For the 10 mm radius, a groove at a distance of 4 mm from the end of the gauge led to a released strain equal to only 82% of the maturation strain.

Thus, a distance not higher than 5 mm between the end of the gauge and the groove is recommended. The measured strain would be slightly lower than the maturation strain α_L (about 95–99%). In the case of very small trees, it is recommended to cut no further than 3 mm from the end of the gauge, and to preferentially use small gauges (2 mm long), as well as a thin saw blade or a cutter to limit the perturbations due to saw cutting (Yoshida and Okuyama 2002). Under these conditions, the measured strain corresponds to 91% of the maturation strain.

Effect of the strain length for fixed distance $D - g$

Based on the previous result, the distance $D - g$ equal to 3 mm for the smallest trees (R = 10 mm), and equal to 5 mm for the others was fixed. The groove depth (d) was now fixed to 10 mm. Figure 12 shows the effect of the length of the strain

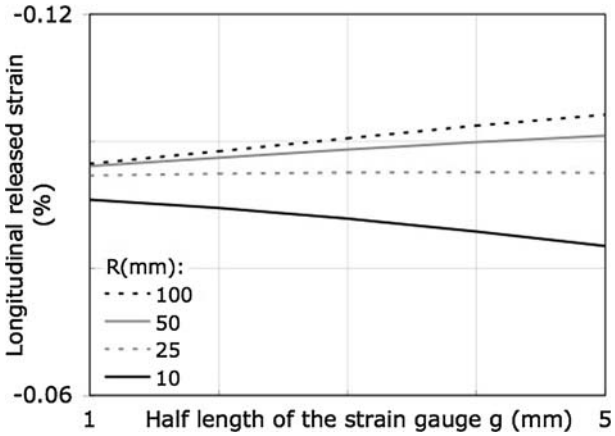

Fig. 12 Effect of the length of the gauge on the longitudinal released strain for a fixed distance $D - g$ for four stem radii (R). d = 10 mm, $D - g$ = 5 mm, except for R = 10 mm for which $D - g$ = 3 mm

gauge on the longitudinal released strain. For trees with a radius between 25 and 100 mm, the released strain slightly increased with the length of the gauge, this effect was higher for bigger stems but in all the cases the variations were small. In the case of very small trees (R = 10 mm), the effect was opposite and accentuated: the longitudinal released strain decreased from 91 to 83% of the maturation strain. The measurement always underestimated the maturation strain in the case of very small trees. Nevertheless, the released strain remained close to α_L: half the length of the strain gauge of 3 mm gave 88, 95, 99 and 100% of the maturation strain for a tree radius of 10, 25, 50 and 100 mm, respectively.

Effect of the strain gauge for a fixed distance D

For a stem radius of 25 mm, the distance between the grooves (D = 6 mm) was fixed and the effect of the gauge length was studied. When the groove depth was less than 2.5 mm, the released strain increased with the gauge length, for deeper grooves, the value became constant and close to the maturation strain α_L. Figure 13 shows that the grooves must be deep enough to have the measured strain independent of the strain gauge length. The next paragraph aims to study the effect of the groove depth on strain measurements.

Effect of groove depth on strain measurements

The released strain increased highly for small groove depth, reached a peak for a groove depth of 4 or 5 mm, and stabilized for deeper grooves (Fig. 14). For the three biggest stems, the peak slightly exceeded the maturation strain α_L, between 104 and 110% of α_L, and the stable value was about 92% of α_L. For the 10 mm radius stem, the released strain remained smaller that the maturation strain, the peak value was about 92% of α_L and the final value about 88%. It can be noticed that for

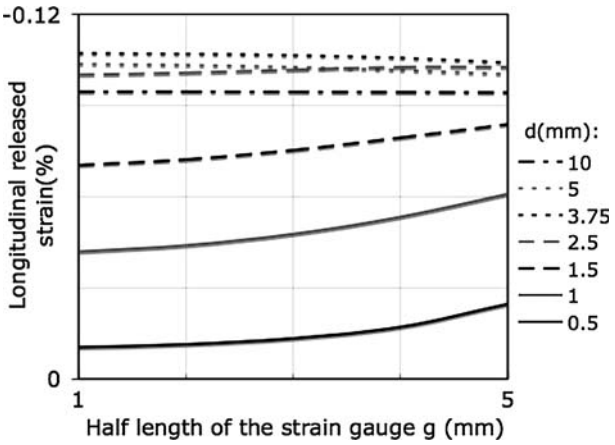

Fig. 13 Effect of the length of the gauge on the longitudinal released strain for a fixed distance D = 6 mm for different groove depths (d). R = 25 mm

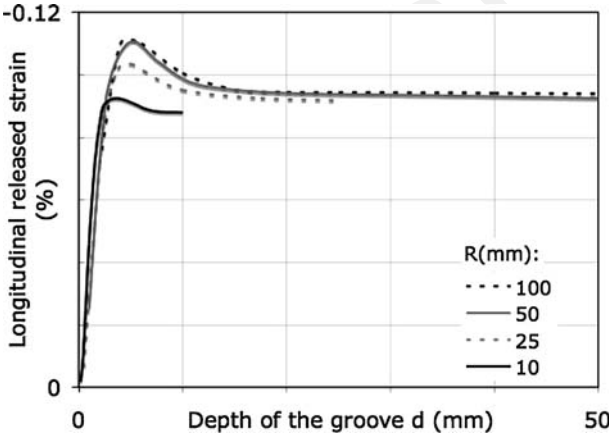

Fig. 14 Effect of groove depth on the longitudinal released strain for four stem radii (R). g = 3 mm, D = 6 mm

the three bigger trees, a groove depth of 10 mm gave an accurate evaluation of α_L. It seems that this method underestimates the maturation strain of very small trees. In the case of a 10 mm radius tree, a groove depth of 4 mm means that 40% of the radius is crosscut: the strain measurement deeply integrates locked strains. This explains the lower value of the released strain.

Conclusion

The finite element model presented in this study allows for simulation of the two-grooves method. The strain gauge measurement is obtained as the relative

displacement of the node corresponding to the upper end of the gauge. The calculations allow comparing the strain gauge measurement to the maturation strain induced in the wood. The numerical tool is effective to simulate some specific situations.

The measurement of the longitudinal maturation strain at the periphery of a tree of radius R is not influenced by the crosscutting of the log if it is made at a distance of at least $3R$ from the measurement. The distance between the end of the gauge and the groove should not be greater than 3 mm in the case of very small trees (R = 10 mm), 5 mm for bigger stems (R = 25, 50, 100 mm). The use of small gauges (2 mm long) is recommended in the case of very small trees.

On a tree of radius 25 mm, for a fixed distance between the grooves of 12 mm, the length of the strain gauge does not influence the strain measurement when the grooves are at least 2.5 mm deep. The measurement is sensible to the groove depth, especially for small groove depths. A depth of 10 mm for the stem radii of at least 25 mm leads to an accurate estimation of the maturation strain. It seems that this method underestimates the maturation strain of very small trees: the strain gauge would measure only about 90% of the maturation strain. This result should be used to correct experimental data on very small trees in order to compare them to data of bigger trees. This suggests that maturation strain in very small trees may be significantly higher than what was measured with this method.

An asymmetric distribution of the maturation strain may influence, to a different degree, the strain measurement all around the tree: the measurement is not much affected by the mechanical situation in the opposite zone. A parameter k was used to describe the internal stress distribution. In the case of a high k value, the maturation strain would be largely underestimated, especially for very small stems. It would be interesting to test other internal stress distributions: the case of changing angular position of the reaction wood zone and/or sudden changes of growth conditions could be investigated using a ring-by-ring description. The geometry of the stem could be modified to investigate the effect of eccentric growth too. This approach could be applied to softwoods taking into account some compression wood zones. It could help to quantify the perturbation on the measurement due to spiral grain for example.

Acknowledgments This work has been partly supported by ANR project "Woodiversity" and the COST Actions E35 and E50.

References

Archer RR (1986) Growth stresses and strains in trees. Springer, Berlin

Fournier M, Chanson B, Thibaut B, Guitard D (1994) Measurement of residual growth strains on the surface of trees, related to their morphology. Observations on different species. Annales des sciences forestières 51(3):249–266 (in French)

Guitard D (1987) Mechanic of wood and composites (in French). Cépaduès-Editions, Toulouse

Jullien D, Yoshida M, Cabrolier P, Gril J (2006a) Measurement of residual strains at stem periphery using the two-grooves method. In: International Conference on integrated approach to wood structure, behaviour and applications. Joint meeting of ESWM and Cost Action E35, Florence, Italy, 15–17 May 2006

Jullien D, Cabrolier P, Gril J (2006b) A finite element model to predict the growth strain release at the periphery of small diameter trees. In: Proceedings of the fifth plant biomechanics conference, vol. 2, 28 August–1 September 2006, Stockholm, Sweden, STFI-Packforsk AB

Kübler H (1959a) Studies on growth stresses in trees – part I: the origin of growth stresses and the stresses in transverse direction. Holz Roh- Werkst 17(1):1–9

Kübler H (1959b) Studies on growth stresses in trees – part II: longitudinal stresses. Holz Roh- Werkst 17(2):44–54

Kübler H (1987) Growth stresses in trees and related wood properties. For Prod Abstr 10(3):62–119

Sassus F (1995) Relation between longitudinal residual strains and physical properties measured on veneer cutting of poplar (clone I214) and beech (*Fagus sylvatica L.*) (in French). In: 8th Seminar on architecture, structure and mechanic of tree, CIRAD, Montpellier, France, LMGC, Université Montpellier 2

Wilson BF, Archer RR (1979) Tree design: some biological solutions to mechanical problems. Bioscience 9:293–298

Yoshida M, Okuyama T (2002) Techniques for measuring growth stress on the xylem surface using strain and dial gauges. Holzforschung 56(5):461–467